J Intell Robot Syst (2014) 73:51–66
DOI 10.1007/s10846-013-9909-4

# Robust Backstepping Control Based on Integral Sliding Modes for Tracking of Quadrotors

**Heriberto Ramirez-Rodriguez · Vicente Parra-Vega · Anand Sanchez-Orta · Octavio Garcia-Salazar**

Received: 5 September 2013 / Accepted: 12 September 2013 / Published online: 27 September 2013


**Abstract** Modern non-inertial robots are usually underactuated, such as fix or rotary wing Unmanned Aerial Vehicles (UAVs), underwater or nautical robots, to name a few. Those systems are subject to complex aerodynamic or hydrodynamic forces which make the dynamic model more difficult, and typically are subject to bounded smooth time-varying disturbances. In these systems, it is preferred a formal control approach whose closed-loop system can predict an acceptable performance since deviations may produce instability and may lead to catastrophic results. Backstepping provides an intuitive solution since it solves underactuation iteratively through slaving the actuated subsystem so as to provide a virtual controller in order to stabilize the underactuated subsystem. However it requires a full knowledge of the plant and derivatives of the state, which it is prone to instability for any uncertainty; and although robust sliding mode has been proposed, discontinuities may be harmful for air- or water-borne nonlinear plants. In this paper, a novel robust backstepping-based controller that induces integral sliding modes is proposed for the Newton–Euler underactuated dynamic model of a quadrotor subject to smooth bounded disturbances, including wind gust and sideslip aerodynamics, as well as dissipative drag in position and orientation dynamics. The chattering-free sliding mode compensates for persistent or intermittent, and possible unmatched state dependant disturbances with reduced information of the dynamic model. Representative simulations are presented and discussed.

This work was supported in Mexico by the Conacyt grants 133346, 133544 and the Conacyt MSc Scholarship 262513.

H. Ramirez-Rodriguez (✉) · V. Parra-Vega · A. Sanchez-Orta
Robotics and Advanced Manufacturing, Research Center for Advanced Studies (CINVESTAV), Industria Metalúrgica 1062, Parque Industrial Ramos Arizpe, Ramos Arizpe, 25903, México
e-mail: heriberto.ramirez@cinvestav.edu.mx

V. Parra-Vega
e-mail: vparra@cinvestav.mx

A. Sanchez-Orta
e-mail: anand.sanchez@cinvestav.mx

H. Ramirez-Rodriguez · V. Parra-Vega · A. Sanchez-Orta
Laboratory of Non-inertial Robots and Man-machine Interfaces, Research Center for Advanced Studies (CINVESTAV), Vía del Conocimiento 201, Parque de Investigación e Innovación Tecnológica, Apodaca, 66600, México

O. Garcia-Salazar
Aerospace Engineering Research and Innovation Center, Autonomous University of Nuevo Leon, Monterrey, Mexico
e-mail: octavio.garcias@uanl.mx

**Keywords** Robust backstepping control · Integral sliding modes · Aerodynamic disturbances · Quadrotor

## 1 Introduction

Unmanned Aerial Vehicles (UAVs) provides a mobility which cannot be covered by humans, for instance, in cluttered or dangerous environments where the human being is at risk. These robot devices are high-end system with outstanding capabilities to accomplish task in remote or human-denied environments. UAVs are expensive and require additional associated systems to operate them safely, typically under human surveillance or in fact under human command because control design for these systems are still subject of research. For the automatic control of UAVs, the closed-loop performance depends implicitly on the quality of the controller, which assumes certain specifications on its associated sensor-feedback, actuation and embedded subsystems. However, apart from the technological side, there are some structural problems that make them very difficult to control, among them: highly coupled nonlinear models, underactuation, possibly non-minimum phase, as well as aerodynamic forces and moments. All these factors claim for a powerful control design, establishing the need to resort on sound control theories to deal with underactuation as well as stabilization under disturbances and model uncertainties.

There are some approaches to deal with those problems, the backstepping approach highlights among them, [1, 2]. Backstepping entails an iterative approach to solve underactuation such that actuated dynamics are surrogated of underactuated dynamics. Unfortunately, this systematic approach requires full knowledge of dynamics, which stands for an extremely difficult assumption to meet in practice for UAVs, [3]. To undertake a partially uncertain underactuated system, extension of backstepping with other schemes has been proposed, such as regressor-based adaptation in [4, 5], function approximation techniques in [6], first or adaptive/second order sliding modes in [7–10]. These schemes exploit the backstepping method to introduce additional stability properties in order to deal with uncertainty, consequently, however resulting in an entangled algorithm that adds complexity to the already involved backsteping algorithm. Other way to deal with underactuation circumventing backstepping is the novel approach to shape iteratively sliding surfaces, or extended error frames, such as [11, 12], or exploiting the high order nonholonomic constraint of a particular plant, [13], however those modified sliding surfaces depend on explicit knowledge of the plant, then it is not evident the typical advantageous of invariance of sliding modes, though its main drawback such as discontinuous control action is still in there. Robust control schemes have been designed based on second order sliding modes in order to estimate the unmatched disturbances [14]. Also, exact differentiation have been proposed to deal with derivatives required to implement backstepping, [15, 16].

In this paper, we are interested in the challenge of resorting on backstepping without adding significant complexity to deal with uncertainties and using a piecewise continuous controller for this purpose. It is proposed a backstepping robust controller, based on integral sliding modes, that shapes a change of coordinates wherein chattering-free sliding mode is enforced, [17], This allows an inner control variable to handle smooth and bounded uncertainties and time-varying disturbances. Simulations are presented for the complete standard quadrotor system in Euler-Lagrange coordinates subject to unknown aerodynamic disturbances such as wind gust and sideslip aerodynamic forces as well as dissipative drag effects, [18–20]. As suggested in [21–23], quadrotor dynamics is written in a convenient canonical form which represents three interconnected subsystems and full details of our proposed approach are presented and discussed.

## 2 The Quadrotor

Modern lightweight quadrotors, show a maneuverability unknown for fixed wing robotic aircrafts, which make them suitable for tasks where human being is inconvenient, risky, dangerous or

costly, besides that their associated infrastructure is minimum in comparison to other UAVs.

The quadrotor is considered as a highly underactuated nonlinear system with fast orientation and slow coupled position dynamics. Having four thrusters for performing hovering and navigation flight, the quadrotor is a challenge for the stabilization in regulation and tracking. Moreover, its low inertia mechanical design is rather simple but tends to instability even when subject to small disturbances in typical flying conditions, such as wind gust and sideslip effects, disturbances on the thrust generation, or other inherent aerodynamic conditions such as ground effect to depart or land.

The position control problem of quadrotors entails solving the underactuation such that orientation dynamics tracks desired position dynamics in order to deliver positioning capabilities at the expense of orientation angles. This establishes the need to resort on sound control theories to design robust automatic controllers that deal with underactuation of the nonlinear dynamic model of the quadrotor under parametric uncertainty and disturbances.

## 3 Control Design

Consider a class of nonlinear underactuated systems subject to smooth bounded disturbances $d_i(t) \in \mathcal{C}^{n-i}$, where $n$ is the number of state variables and $n-i$ is the relative degree of the disturbance with respect to the physical control signal, for $i = 2, 4, \ldots, n$. This class of system can be written as follows

$$\dot{x}_1 = x_2 \tag{1}$$

$$\dot{x}_2 = f_2(x) + g_2(x)\varphi_2(x_3) + d_2(t) \tag{2}$$

$$\vdots$$

$$\dot{x}_i = x_{i+1} \tag{3}$$

$$\dot{x}_{i+1} = f_{i+1} + g_{i+1}(x)\varphi_{i+1}(x_{i+2}) + d_{i+1}(t) \tag{4}$$

$$\vdots$$

$$\dot{x}_{n-1} = x_n \tag{5}$$

$$\dot{x}_n = f_n(x) + g_n(x)u + d_n(t) \tag{6}$$

where $x_i \in R^{n_i}$ stands for the state space representation of the system, $f_i(x) \in R^{n_i}$ stands for the flow dynamics of the $x_i$ coordinate, $g_i(x) \in R^{n_i \times n_i}$ is a non singular matrix, $\varphi_i(x) \in R^{n_i}$ is a smooth vector field, for $i = 2, 4, \ldots, n$, such that its Jacobians, $J_i(x) \triangleq \frac{\partial \varphi_{i-1}(x_i)}{\partial x_i}$ are nonsingular (this assumption is fulfilled by the dynamic model of quadrotor [23]), with $n$ an even number.[1]

### 3.1 Problem Statement

The control problem can be stated as follows

> *Given a desired function $x_d$ for the unactuated coordinate $x_1$, design an exogenous piecewise continuous control input $u$ so as to $\|x_d - x_1\|, \|\dot{x}_d - \dot{x}_1\| \to 0$ as $t \to \infty$ locally asymptotically, subject to parametric uncertainties in $f_i(x)$ and unknown time-varying disturbances $d_i(t)$ for the system (1–6), with all coordinates stabilized.*

We will design $u$ using the backstepping scheme parameterized in a novel error coordinate system, useful to induce integral sliding modes to compensate for uncertainties and disturbances, in order to satisfy the above problem. This novel extension of backstepping becomes fundamental to compensate for unmatched uncertainties as well as matched ones.

### 3.2 Design of the Integral Sliding Mode Controller Based on Backstepping

The system (1–6) can be regarded as a chain of interconnected second order subsystems of the form (3–4), coupled by virtual controls $\varrho_{i+1}$ that converge to the desired value $\varphi_{i+1}(x_{i+2})$; in this way, if the error variables are defined as

$$\zeta_i \triangleq \varrho_{i-1} - \varphi_{i-1}(x_i) \tag{7}$$

$$\zeta_{i+1} \triangleq \varrho_i - x_{i+1} \tag{8}$$

with $\varrho_0 = x_d$ and $\varphi_0(x_1) = x_1$, then $\varrho_{i-1}$ becomes the desired reference for $\varphi_{i-1}(x_i)$ and $\varrho_{i+1}$ becomes the control input of the unactuated subsys-

[1] If $n$ were odd, the control scheme is valid with a straightforward modification, as will be shown in the main result at the end of this section.

tem, such that $\zeta_i, \zeta_{i+1} \to 0$. We aim at writing an equivalent representation of the system in error coordinates $S_{ri} = \dot{\zeta}_i - \dot{\zeta}_{ir}$, where $\dot{\zeta}_{ir}$ is a nominal reference. We show that this can be obtained by defining a virtual control $\varrho_{i+1} = \varphi_{i+1}(x_{i+2})$, over a novel parametrization, such that a sliding surface depends on the error tracking variables $\Delta x$ and $\Delta \dot{x}$. In this way, for each subsystem it is proposed the following lemma:

**Lemma 1** *Let Eqs. 3–4 be a subsystem of Eqs. 1–6, for $i = 1, 3, ..., n-1$. Consider the following virtual controllers*

$$\varrho_i = J_i^{-1}(x)\dot{\bar{\varrho}}_{i-1} \tag{9}$$

$$\varrho_{i+1} = \left[J_i(x)g_{i+1}\right]^{-1}\left(K_{di}S_{ri} - \overline{Y}_{ri}\right) \tag{10}$$

*where the Jacobian matrices $J_i(x) \triangleq \frac{\partial \varphi_{i-1}(x_i)}{\partial x_i}$ and $g_{i+1}(x)$ were assumed nonsingular, the nominal variable $\overline{Y}_{ri} = Y_{ri} - \delta_i(d)$ does not contain information about the bounded disturbances, given by $\delta_i(d) \leq \overline{\delta}_i$, for $\overline{\delta}_i \in \mathcal{R}_+$. The derivative of i-th virtual control $\dot{\bar{\varrho}}_{i-1}$ does not contain the disturbance terms. $Y_{ri}$ is given by*

$$Y_{ri} = \ddot{\zeta}_{ir} - \ddot{\varrho}_{i-1} + J_i(x)\, f_{i+1}(x) + \delta_i(d) - \dot{J}_i\,(\zeta_{i+1} - \varrho_i) \tag{11}$$

*where the nominal variable $\dot{\zeta}_{ir}$ is defined by*

$$\dot{\zeta}_{ir} = -\alpha_i\zeta_i + S_{di} - \gamma_i\sigma_i \tag{12}$$

$$\dot{\sigma}_i = \text{sign}(S_{qi}) \tag{13}$$

$$S_{qi} = S_i - S_{di} \tag{14}$$

$$S_i = \dot{\zeta}_i + \alpha_i\zeta_i \tag{15}$$

$$S_{di} = S_i(t_0)e^{-\kappa_i(t-t_0)} \tag{16}$$

*where* sign$(\cdot)$ *stands for the signum function, for positive feedback gains $\alpha_i$, $\gamma_i$ and $\kappa_i$. Then, local exponential tracking is obtained such that $x_i \to x_{di}$ and $\dot{x}_i \to \dot{x}_{di}$, with all closed-loop signals bounded.*

*Proof* (Boundedness of closed-loop signals) Define a virtual control $\varrho_i = x_{i+1}$, such that the following subsystem is obtained:

$$\dot{\zeta}_i = \dot{\varrho}_{i-1} - \varrho_i \tag{17}$$

Now, let $\zeta_{i+1} = \varrho_i - x_{i+1}$ define an error variable useful to write an equivalent system for Eqs. 3–4 as follows

$$\dot{\zeta}_i = \dot{\varrho}_{i-1} - J_i(x)\,(\varrho_i - \zeta_{i+1}) \tag{18}$$

$$\dot{\zeta}_{i+1} = \dot{\varrho}_i - f_{i+1}(x) - g_{i+1}(x)\varrho_{i+1} - d_{i+1}(t) \tag{19}$$

Then, Eqs. 18–19 can be written in terms of error coordinate $S_{ri}$ as follows

$$\dot{S}_{ri} = -J_i(x)g_{i+1}(x)\varrho_{i+1} - Y_{ri} - J_i(x)d_{i+1}(t) \tag{20}$$

Substituting Eq. 10 into Eq. 20, one obtains the following closed loop equation

$$\dot{S}_{ri} = -K_{di}S_{ri} - \delta_i(d) - J_i(x)d_{i+1}(t) \tag{21}$$

That is, first subsystem has been written in error coordinates $S_{ri}$. Then, it remains to proof that Eq. 21 is bounded and for certain tuning of feedback gains and initial conditions, an sliding mode is induced at $S_{qi} = 0$ for all time. To this end, and following [17], let $V_{i+1} = \frac{1}{2}S_{ri}^T S_{ri}$ be a quadratic function, whose time derivative along Eq. 21 becomes

$$\begin{aligned}\dot{V}_{i+1} &= S_{ri}^T(-K_{di}S_{ri} - \delta_i(d) - J_i(x)d_{i+1}(t)) \\ &\leq -\|S_{ri}\|\left(\lambda_{\min}\{K_{di}\}\|S_{ri}\| - \overline{\delta}_i - \bar{J}_{di}\right)\end{aligned} \tag{22}$$

where $\|J_i(x)d_{i+1}(t)\| \leq \bar{J}_{di} > 0$ and $\|\delta_i(d)\| \leq \bar{\delta}_i$, for $\bar{\delta}_i > 0$. Then, for a large enough $K_{di}$, such that $\lambda_{\min}\{K_{di}\}\|S_{ri}\| > \bar{\delta}_i + \bar{J}_{di}$, there exists a finite time $t_i$ such that $\|S_{ri}\| \leq C_{sri} = \left(\left(\overline{\delta}_i + \bar{J}_{di}\right)/\lambda_{\min}\{K_{di}\}\right)$. Moreover, $\dot{S}_{ri}$ is bounded by $C_{\dot{s}ri} = \lambda_{\max}\{K_{di}\}C_{sri} + \overline{\delta}_i + \bar{d}_{i+1}$. So far, we have proved only that all closed-loop signals are bounded for the subsystem (21). □

*Proof* (Integral Sliding Mode) Using Eqs. 12, 14 and 15, variable $S_{ri}$ becomes

$$S_{ri} = S_{qi} + \gamma_i\sigma_i \tag{23}$$

In order to prove that Eq. 23 yields a sliding mode at $S_{qi} = 0$, consider the time derivative of $V_{qi} = \frac{1}{2}S_{qi}^T S_{qi}$ along the derivative of Eq. 23:

$$\begin{aligned}\dot{V}_{qi} &= -S_{qi}^T\gamma_i\text{sign}(S_{qi}) + S_{qi}^T\dot{S}_{ri} \\ &\leq -\lambda_{\min}\{\gamma_i\}|S_{qi}| + |S_{qi}||\dot{S}_{ri}|\end{aligned}$$

$$\leq -\lambda_{\min}\{\gamma_i\}|S_{qi}| + C_{\dot{s}ri}|S_{qi}|$$

$$\leq -\mu_i|S_{qi}| \tag{24}$$

where $\mu_i = \lambda_{\min}\{\gamma_i\} - C_{\dot{s}ri}$. If $K_{di}$ and $\gamma_i$ are chosen such that $\mu_i > 0$, then the sliding mode condition $S_{qi}^T \dot{S}_{qi} < -\mu_i|S_{qi}|$ is fulfilled for a sliding mode at $S_{qi} = 0\ \forall t \geq t_{si} \leq |S_{qi}(t_0)|/\mu_i$. Moreover, $S_{qi} = 0$ for all time due to the reaching phase is removed by the exponentially vanishing term $S_{di}$. This leads to conclude the asymptotic convergence of $\zeta_i$ and $\dot{\zeta}_i$, implying by Eqs. 9 and 18 that $\zeta_{i+1} \to 0$ asymptotically. □

Based on the backstepping approach and Lemma 1, the following $k$-step procedure is proposed for the subsystem (1–6):

**Step 1**: Define the virtual control $\varrho_2 = \varphi_2(x_3)$ and let $x_{d1}$ be the desired reference for $x_1$, for the subsystem:

$$\dot{x}_1 = x_2 \tag{25}$$

$$\dot{x}_2 = f_2(x) + g_2(x)\varrho_2 + d_2(t) \tag{26}$$

According to Lemma 1, subsystem (25–26) can be represented in error coordinates as follows:

$$\dot{S}_{r1} = -g_2(x)\varrho_2 - Y_{r1} - d_2(t) \tag{27}$$

Defining

$$\varrho_1 = \dot{x}_{di} \tag{28}$$

$$\varrho_2 = g_2^{-1}(x)\left(K_{d1}S_{r1} - \overline{Y}_{r1}\right) \tag{29}$$

the asymptotic convergence $x_1 \to x_{d1}$, $\dot{x}_1 \to \dot{x}_{d1}$ and $x_2 \to \varrho_1$ is ensured.

**Step 2**: Let $\varrho_4 = \varphi_4(x_5)$ be a virtual control and $\varrho_2$ the reference for $x_3$, in the subsystem:

$$\dot{x}_3 = x_4 \tag{30}$$

$$\dot{x}_4 = f_4(x) + g_4(x)\varrho_4 + d_4(t) \tag{31}$$

Lemma 1 suggests that the subsystem (30–31) can be written as follows:

$$\dot{S}_{r3} = -J_3(x)g_4(x)\varrho_4 - Y_{r3} - J_3(x)d_4(t) \tag{32}$$

Now, consider the virtual control

$$\varrho_3 = J_3^{-1}(x)\dot{\bar{\varrho}}_2 \tag{33}$$

$$\varrho_4 = \left[J_3(x)g_4(x)\right]^{-1}\left(K_{d3}S_{r3} - \overline{Y}_{r3}\right) \tag{34}$$

that stabilizes states $x_3$ and $x_4$. In order to analyze the stability of subsystem (27) and (32), with control law (28), (29), (33) and (34), it is proposed the quadratic function $V_2 = \frac{1}{2}S_{r1}^T S_{r1} + \frac{1}{2}S_{r3}^T S_{r3}$. Notice that actually in Eq. 27, we have $\varrho_2 - \zeta_3$ instead of $\varrho_2$, so taking this into account, the time derivative of $V_2$ becomes,

$$\begin{aligned}\dot{V}_2 &= S_{r1}^T(-K_{d1}S_{r1} + g_2(x)\zeta_3 - \delta_1(d) \\ &\quad - d_2(t)) + S_{r3}^T(-K_{d3}S_{r3} - \delta_3(d) \\ &\quad - J_3(x)d_4(t)) \\ &\leq -\|S_{r1}\|\left(\lambda_{\min}\{K_{d1}\}\|S_{r1}\| - C_{g2} - \bar{\delta}_1\right. \\ &\quad \left. - \bar{d}_2\right) - \|S_{r3}\|\left(\lambda_{\min}\{K_{d3}\}\|S_{r3}\|\right. \\ &\quad \left. - \bar{J}_{d3} - \bar{\delta}_3\right)\end{aligned} \tag{35}$$

where it is assumed that $\|g_2(x)\zeta_3\| \leq C_{g2}$, $\|J_3(x)d_4(t)\| \leq \bar{J}_{d3}$ for $C_{g2}, \bar{J}_{d3} > 0$. If we consider that $\zeta_3(t_0)$ belongs to a bounded set with radius $r > 0$ centered in the origin $(S_{r1}, S_{r3}) = (0, 0)$, and given that $x_{d3}$ is smooth, there exist large enough feedback gains $K_{d1}$ and $K_{d3}$ such that, $\lambda_{\min}\{K_{d1}\}\|S_{r1}\| > C_{g2} + \bar{\delta}_1 + \bar{d}_2$ and $\lambda_{\min}\{K_{d3}\}\|S_{r3}\| > \bar{J}_{d3} + \bar{\delta}_3$, then $\dot{V}_2 < 0$. In this condition, we can assume that $\zeta_3$ remains into the bounded set afterwards. In this way $S_{r1}$ and $S_{r3}$ remain bounded and the second part of the proof of Lemma 1 is valid for $i = 1, 3$. This guarantees the convergence of $x_1 \to x_{d1}, \dot{x}_1 \to \dot{x}_{d1}, x_2 \to \varrho_1, x_3 \to \varrho_2$ and $x_4 \to \varrho_3$.

**Step *k***: Define the virtual control $\varrho_{2k} = \varphi_{2k}(x_{2k+1})$ and let $\varrho_{2k-2}$ be the reference for $\varphi_{2k-2}(x_{2k-1})$ of the following subsystem:

$$\dot{x}_{2k-1} = x_{2k} \tag{36}$$

$$\dot{x}_{2k} = f_{2k}(x) + g_{2k}(x)\varrho_{2k} + d_{2k}(t) \tag{37}$$

for $k = 1, 2, \ldots, n/2$. According to Lemma 1, subsystem (36–37) can be written as follows:

$$\dot{S}_{r_{2k-1}} = -J_{2k-1}(x)g_{2k}(x)\varrho_{2k} - Y_{r_{2k-1}} - J_{2k-1}(x)d_{2k}(t) \tag{38}$$

such that by considering the following virtual control

$$\varrho_{2k-1} = J_{2k-1}^{-1}(x)\dot{\bar{\varrho}}_{i-1} \tag{39}$$

$$\varrho_{2k} = \left[J_{2k-1}(x)g_{2k}(x)\right]^{-1} \times \left(K_{d_{2k-1}}S_{r_{2k-1}} - \overline{Y}_{r_{2k-1}}\right) \tag{40}$$

the closed loop stabilizes the states $x_{2k-1}$ and $x_{2k}$. To show this, consider the subsystem given by $S_{r1}$, $S_{r3}$, …, $S_{r_{2k-3}}$ and $S_{r_{2k-1}}$, with the control law $\varrho_2$, $\varrho_4$, …, $\varrho_{2k-2}$ and $\varrho_{2k}$. Now, let $V_{2k-2} = \frac{1}{2}\sum_{m=1}^{k} S_{r(2m-1)}^T S_{r(2m-1)}$ be a quadratic function. Taking the time derivative of $V_{2k-2}$ along its solution (38), one obtains

$$\begin{aligned}
\dot{V}_{2k-2} = {} & S_{r1}^T\big(-K_{d1}S_{r1} + g_2(x)\zeta_3 - \delta_1(d) \\
& - d_2(t)\big) + S_{r3}^T\big(-K_{d3}S_{r3} + g_4(x)\zeta_5 \\
& - \delta_3(d) - J_3(x)d_4(t)\big) + \ldots \\
& + S_{r_{2k-3}}^T\big(-K_{d_{2k-3}}S_{r_{2k-3}} \\
& + g_{2k-2}(x)\zeta_{2k-1} - \delta_{2k-3}(d) \\
& - J_{2k-3}(x)d_{2k-2}(t)\big) \\
& + S_{r_{2k-1}}^T\big(-K_{d_{2k-1}}S_{r_{2k-1}} - \delta_{2k-1}(d) \\
& - J_{2k-1}(x)d_{2k}(t)\big) \\
\leq {} & -\|S_{r1}\|\big(\lambda_{\min}\{K_{d1}\}\|S_{r1}\| \\
& - C_{g2} - \overline{\delta}_1 - \bar{d}_2\big) \\
& - \|S_{r3}\|\big(\lambda_{\min}\{K_{d3}\}\|S_{r3}\| \\
& - C_{g4} - \bar{J}_{d3} - \overline{\delta}_3\big) - \\
& \vdots \\
& - \|S_{r_{2k-3}}\|\big(\lambda_{\min}\{K_{d_{2k-3}}\}\|S_{r_{2k-3}}\| \\
& - C_{g2k-2} - \bar{J}_{d2k-3} - \overline{\delta}_{2k-3}\big) \\
& - \|S_{r_{2k-1}}\|\big(\lambda_{\min}\{K_{d_{2k-1}}\}\|S_{r_{2k-1}}\| \\
& - \bar{J}_{2k-1} - \overline{\delta}_{2k-1}\big)
\end{aligned} \tag{41}$$

where it is assumed that $\|g_m(x)\zeta_{m+1}\| \leq C_{gm}$, $\|J_{m-1}(x)d_m(t)\| \leq \bar{J}_{dm-1}$ for $C_{gm}, \bar{J}_{dm-1} > 0$ and $m = 2, 4, \ldots, 2k-2$. Assuming small initial errors of $\zeta_3$, $\zeta_5$, …, $\zeta_{2k-3}$, $\zeta_{2k-1}$ such that, this initial state belongs to a bounded set with radius $r > 0$ centered in the origin $S_{r1}$, $S_{r3}, \ldots, S_{r_{2k-3}}, S_{r_{2k-1}} = 0$. There exists large enough feedback gains $K_{d1}$, $K_{d3}$, …, $K_{d_{2k-3}}$ and $K_{d_{2k-1}}$, such that, $\lambda_{\min}\{K_{d1}\}\|S_{r1}\| > C_{g2} + \bar{\delta}_1 + \bar{d}_2, \lambda_{\min}\{K_{dm-1}\}\|S_{rm-1}\| > C_{gm} + \bar{J}_{dm-1} + \bar{\delta}_{m-1}$ for $m = 4, 6, \ldots, 2k-2$ and $\lambda_{\min}\{K_{d2k-1}\}\|S_{r2k-1}\| > \bar{J}_{d2k-1} + \bar{\delta}_{2k-1}$, then $\dot{V}_{2k-2} < 0$. Now, this shows that $\zeta_3$, $\zeta_5$, …, $\zeta_{2k-3}$, $\zeta_{2k-1}$ remain into the bounded set afterwards such that $S_{r1}, S_{r3}, \ldots, S_{r_{2k-3}}, S_{r_{2k-1}}$ and $S_{r3}$ remain bounded. Now, provided that the second part of the proof of Lemma 1 is valid for $i = 1, 3, \ldots, 2k-3, 2k-1$, then it guarantees locally exponentially the convergence of $x_1 \to x_{d1}$, $\dot{x}_1 \to \dot{x}_{d1}$, $x_2 \to \varrho_1$, $x_3 \to \varrho_2$, $x_4 \to \varrho_3, \ldots, x_{2k-1} \to \varrho_{2k-2}$, $x_{2k} \to \varrho_{2k-1}$.

### 3.3 Main Result

Now we are ready to present the main result.

**Theorem 1** *Consider the system (1–6) subject to parametric uncertainty and smooth continuous bounded disturbances $d_i(t)$. Let $\bar{d}_i \in \mathcal{R}_+$ be the bounds of the disturbances, such that, $\|d_i\| \leq \bar{d}_i$ for $i = 2, 4, \ldots, n$. Then, with a chain of $n/2$ virtual controls based on Integral Sliding Mode Control given by Eqs. 9 and 10, the error variables converge locally asymptotically to the origin.*

*Proof* Based on the result of the $k$-th step procedure when $k = n/2$, the following control is obtained:

$$\varrho_1 = \dot{x}_{d1} \tag{42}$$

$$\varrho_2 = \left[J_1(x)g_2(x)\right]^{-1}\left(K_{d1}S_{r1} - \overline{Y}_{r1}\right) \tag{43}$$

$$\varrho_3 = J_3^{-1}(x)\dot{\bar{\varrho}}_2 \tag{44}$$

$$\varrho_4 = \left[J_3(x)g_4(x)\right]^{-1}\left(K_{d3}S_{r3} - \overline{Y}_{r3}\right) \tag{45}$$

$$\vdots$$

$$\varrho_{n-3} = J_{n-3}^{-1}(x)\dot{\bar{\varrho}}_{n-4} \tag{46}$$

$$\varrho_{n-2} = \left[J_{n-3}(x)g_{n-2}(x)\right]^{-1}\left(K_{d_{n-3}}S_{r_{n-3}} - \overline{Y}_{r_{n-3}}\right) \tag{47}$$

$$\varrho_{n-1} = J_{n-1}^{-1}(x)\dot{\bar{\varrho}}_{n-2} \tag{48}$$

$$u = \left[J_{n-1}(x)g_n(x)\right]^{-1}\left(K_{d_{n-1}}S_{r_{n-1}} - \overline{Y}_{r_{n-1}}\right) \tag{49}$$

The chain of virtual controls (42–49) clearly guarantees the convergence of $\zeta_1, \dot{\zeta}_1, \zeta_2, \zeta_3, \dot{\zeta}_3, \zeta_4, \ldots, \zeta_{n-3}, \dot{\zeta}_{n-3}, \zeta_{n-2}, \zeta_{n-1}, \dot{\zeta}_{n-1}, \zeta_n \to 0$. □

*Remark 1* Notice that although time-varying bounded smooth disturbances are not affine to the control input $u$, a class of disturbances are rejected with a chattering-free controller. Now, let us consider the case when there is an additional state $x_{n+1}$ as follows,

$$\dot{x}_1 = x_2 \tag{50}$$

$$\dot{x}_2 = f_2(x) + g_2(x)\varphi_2(x_3) + d_2(t) \tag{51}$$

$$\vdots$$

$$\dot{x}_{n-1} = x_n \tag{52}$$

$$\dot{x}_n = f_n(x) + g_n(x)\varphi_n(x_{n+1}) + d_n(t) \tag{53}$$

$$\dot{x}_{n+1} = v \tag{54}$$

The, system (50–54) can be stabilized by the virtual controls (42–49), with $\varrho_n = u$, such that $v$ can be designed with the classical backstepping approach as follows

$$v = J_{n+1}^{-1}(x)\left(A_{n+1}\zeta_{n+1} + g_n^T(x)S_{r_{n-1}} + \dot{\bar{\rho}}_n\right) \tag{55}$$

where $\dot{\bar{\rho}}_n$ does not depends on the disturbances. This controller guarantees, in virtue of Theorem 1, the convergence of $\zeta_i, i = 1, 2, ..., n$ to zero, with all closed-loop signals bounded, despite unmatched disturbances $d_i(t)$.

*Remark 2* Notice that in Eq. 10, the term $\overline{Y}_{ri}$ implies the second time derivative of reference $\varrho_{i-1}$, necessary for $i = 3, 5, \ldots, n-1$, which involves the time derivative of signum function, which evidently does not exist, this arises as consequence of introducing a signum function to induce a sliding mode, which is typical in particular for backstepping sliding modes. This fact is present in a number of relevant contribution in the literature, however it lacks of a proper study, or it is simply overlooked. In our case, the first derivative of $x_{di}$ can be computed, since the integral of signum function is involved, but not the second one. In order to overcome this drawback, or essentially this pitfall, a signum function approximation can be used. That is $\text{sign}(S_{qi}) \approx \tanh(\beta S_{qi})$, with $\beta > 0$ in $\ddot{\varrho}_{i-1}$, but $\text{sign}(S_{qi})$ is used in $\varrho_{i-1}, \dot{\varrho}_{i-1}$ to preserve a quasi-sliding mode to guarantee prescribed precision. To show this, let $\dot{V}_{qi}$ become

$$\begin{aligned}\dot{V}_{qi} &= -S_{qi}^T\gamma_i\tanh(\beta S_{qi}) + S_{qi}^T\dot{S}_{ri} \\ &= -S_{qi}^T\gamma_i\text{sign}(S_{qi}) + S_{qi}^T\dot{S}_{ri} \\ &\quad - S_{qi}^T\gamma_i\left(\tanh(\beta S_{qi}) - \text{sign}(S_{qi})\right) \\ &\leq -\lambda_{\min}\{\gamma_i\}|S_{qi}| + |S_{qi}||\dot{S}_{ri}| + \lambda_{\max}\{\gamma_i\}\Delta s|S_{qi}| \\ &\leq -(\mu_i - \mu_0)|S_{qi}|\end{aligned} \tag{56}$$

where $\mu_0 = \lambda_{\max}\{\gamma_i\}\Delta s$ and $0 <| \Delta s |< 1 \ \forall \ S_{qi}$. When $\mu_0 > \mu_i$, $\dot{V}_{qi} > 0$ and $S_{qi}$ increase and $\Delta s \to 0$, such that there exist a time $t_{\Delta s}$ where $\dot{V}_{qi} < 0$, thus $S_{qi}$ remains on a vicinity of the origin, the size of this vicinity is determined by the parameter $\beta$, in this case it is said that a quasi-sliding mode is induced. However, notice that this problem is not present in control law $u$, because its time derivative is not needed, so in this case the signum function can be implemented.

## 4 Application to a Quadrotor

### 4.1 Quadrotor Dynamics

Consider the following dynamic model of the quadrotor rotorcraft,

$$mR_t^T\ddot{\xi} + k_tR_t^T\dot{\xi} + mR_t^TG = F + d_\xi(t) \tag{57}$$

$$\begin{aligned}I_TR_r\ddot{\eta} + I_T\left(\frac{\partial R_r}{\partial\phi}\dot{\phi} + \frac{\partial R_r}{\partial\theta}\dot{\theta}\right)\dot{\eta} + k_rR_r\dot{\eta} \\ + (R_r\dot{\eta}) \times (I_rR_r\dot{\eta}) = \tau + d_\eta(t)\end{aligned} \tag{58}$$

where $m$ and $I_T = \text{diag}\left(I_x, I_y, I_z\right)$ are the mass and the inertia matrix of the quadrotor, respectively; matrices $k_t > 0$ and $k_r > 0$ contain

aerodynamic dissipative friction coefficients. Vector $G = \begin{bmatrix} 0 & 0 & g \end{bmatrix}^T$ stands for the acceleration due to the gravitational field of Earth, $\xi = \begin{bmatrix} x & y & z \end{bmatrix}^T$ and $\eta = [\phi \ \theta \ \psi]^T$ represent position and orientation in world coordinates, respectively. Exogenous $F$ and $\tau$ are the control forces and moments generated by the rotors of the aerial vehicle,

$$F = \begin{bmatrix} 0 \\ 0 \\ \sum_{i=1}^{4} F_i \end{bmatrix}, \ \tau = \begin{bmatrix} d\,(F_2 - F_4) \\ d\,(F_3 - F_1) \\ c \sum_{i=1}^{4} (-1)^{i+1} F_i \end{bmatrix}$$

where $d$ is the distance from the center of mass to the rotor shafts and $c$ is the drag coefficient. Rotation matrices are defined as follows, for the usual notation of $c_a = cos(a)$ and $s_b = sin(b)$,

$$R_t = \begin{bmatrix} c_\phi c_\psi & s_\phi s_\theta c_\psi - c_\phi s_\psi & c_\phi s_\theta c_\psi + s_\phi s_\psi \\ c_\theta s_\psi & s_\phi s_\theta s_\psi + c_\phi c_\psi & c_\phi s_\theta s_\psi - s_\phi c_\psi \\ -s_\phi & s_\phi c_\theta & c_\phi c_\theta \end{bmatrix}$$

$$R_r = \begin{bmatrix} 1 & 0 & -s_\theta \\ 0 & c_\phi & c_\theta s_\phi \\ 0 & -s_\phi & c_\phi c_\theta \end{bmatrix}$$

which stand for the transformation and rotation velocity matrices, respectively, between the inertial reference frame and the body reference frame. Terms $d_\xi(t) = \begin{bmatrix} d_x & d_y & d_z \end{bmatrix}^T$ and $d_\eta(t) = \begin{bmatrix} d_\phi & d_\theta & d_\psi \end{bmatrix}^T$ model smooth bounded disturbances, possibly time-varying and state dependant. Now, the aerodynamic forces, moments and state-dependant aerodynamical disturbances are presented.

#### 4.1.1 Aerodynamic Disturbance Force

Consider axes according to the wind direction velocity vector as the aerodynamic frame, then two axes arises from the rotation matrix $W : \mathcal{B} \to \mathcal{A}$ where $\mathcal{B}$ represents the frame attached to the body, and

$$W = \begin{pmatrix} c_\alpha c_\beta & s_\beta & s_\alpha c_\beta \\ -c_\alpha s_\beta & c_\beta & -s_\alpha s_\beta \\ -s_\alpha & 0 & c_\alpha \end{pmatrix}$$

where $\alpha$ is the angle of attack and $\beta$ stands for the sideslip angle, [18]. The aerodynamic forces produced during the hovering flight are written as follows

$$d_\xi = W^T \begin{pmatrix} L \\ Y \\ D \end{pmatrix} = W^T \begin{pmatrix} \frac{1}{2}\rho_a v_r^2 S c_L \\ \frac{1}{2}\rho_a v_r^2 S c_Y \\ \frac{1}{2}\rho_a v_r^2 S c_D \end{pmatrix}$$

for $L$, $Y$, and $D$ the lift, side force, and drag coefficients of aerodynamic forces, respectively. $S$ represents the platform area of one blade of the vehicle, and $c_D$, $c_Y$, $c_L$ stand for the aerodynamical non-dimensional coefficients of drag, sideforce and lift, respectively, [20].

#### 4.1.2 Gyroscopic and Aerodynamic Moment Disturbances

The moments acting on the vehicle from aerodynamical disturbances are defined as follows

$$d_\eta = d_{\eta g} + d_{\eta a}$$

where $d_{\eta g}$ stands for the *Gyroscopic Moment* generated by the rotation of the airframe and the four rotors, described by

$$\begin{aligned} d_{\eta g} &= \sum_{i=1}^{4} (-1)^{i+1} I_{r_i} [\Omega \times e_z \omega_i)] \\ &= \begin{pmatrix} q(I_{r_1}\omega_{r_1} - I_{r_2}\omega_{r_2} + I_{r_3}\omega_{r_3} - I_{r_4}\omega_{r_4}) \\ p(-I_{r_1}\omega_{r_1} + I_{r_2}\omega_{r_2} - I_{r_3}\omega_{r_3} + I_{r_4}\omega_{r_4}) \\ 0 \end{pmatrix} \end{aligned}$$

for $I_{r_i}$ the moment of inertia of $i$-th rotor, $e_z = [0\ 0\ 1]^T$, and $\omega_i$ denote the angular velocity of the rotor $i$, with $i$=1, 2, 3, 4, respectively.

The *Aerodynamic Moment* $d_{\eta a}$ is modeled by

$$d_{\eta a} = \begin{pmatrix} \Gamma_l \\ \Gamma_m \\ \Gamma_n \end{pmatrix} = \begin{pmatrix} \frac{1}{2}\rho_a v_r^2 S b\, c_l \\ \frac{1}{2}\rho_a v_r^2 S \bar{c} c_m \\ \frac{1}{2}\rho_a v_r^2 S b\, c_n \end{pmatrix}$$

where $\Gamma_l$, $\Gamma_m$ and $\Gamma_n$ stand for the aerodynamic rolling, pitching and yawing moments, respectively; coefficients $\bar{c}$ and $b$ are the chord and the span of a blade, respectively, and $c_l$, $c_m$ and $c_n$ are aerodynamical non-dimensional coefficients

of the aerodynamic rolling, pitching and yawing moments, respectively, [20]. Finally, $\alpha$, $v_r$ and $\beta$ as well as the yaw moment, due to sideslip, are derived along the longitudinal and directional motions.

#### 4.1.3 Longitudinal Motion

From Fig. 1, the quadrotor turns in the direction of the wind gust, for $v_o$ is the freestream velocity, $v_i$ represents the induced velocity and is directed opposite to the thrust, $\alpha_o$ stands for the freestream angle of attack, and $\alpha$ is the angle of attack, and $v_r$ is the resultant velocity in the propeller slipstream, [19]. Analyzing the wind velocity vectors from Fig. 1, it can be established that the resultant wind velocity in forward flight, results an angle of attack as follows

$$v_r = \sqrt{(v_o \sin\alpha_o)^2 + (v_o \cos\alpha_o + v_i)^2} \tag{59}$$

$$\alpha = \arctan\left(\frac{v_o \sin\alpha_o}{v_o \cos\alpha_o + v_i}\right) \tag{60}$$

For hover flight, thrust is $T = \dot{m} v_v$, for $\dot{m} = \rho_a A v_r$ the mass flow rate where $A$ stands for the rotor disk area, $\rho$ denotes the air density, and $v_v = 2v_i$ the velocity in the vena contracta. Taking $v_o = 0$ and (59), the induced velocity in hover regime becomes $v_h = \sqrt{\frac{T}{2\rho_a A}}$.

#### 4.1.4 Directional motion

In flight conditions, it is desired to maintain the sideslip angle at zero to avoid yawing moment (Fig. 2). Nevertheless, it arises in presence of wind

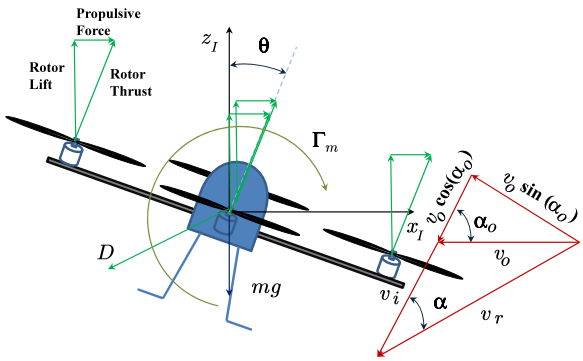


**Fig. 1** Quadrotor cruise in presence of wind gust disturbance

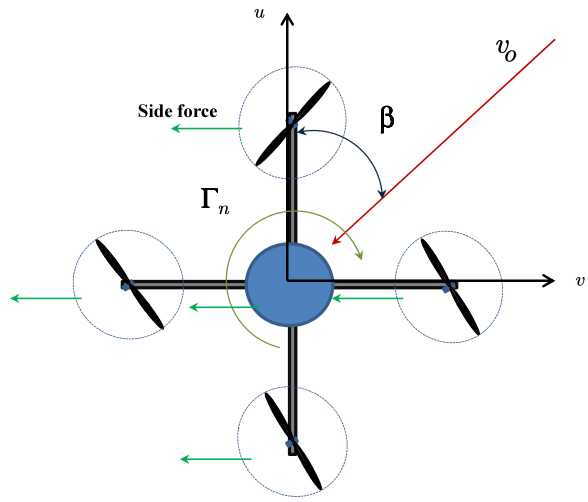


**Fig. 2** Sideslip angle and yawing moment

gust, [18], for a freestream velocity $v_o$. In this condition, the sideslip angle can be described as

$$\beta = \arcsin\left(\frac{v}{v_o}\right) \tag{61}$$

In virtue of (61), it results a yawing moment given by

$$\Gamma_n = c_{n_\beta} \frac{\rho_a v^2}{2} S b \beta \tag{62}$$

where $c_{n_\beta} \approx (c_{n_\beta})_{\text{Propellers}} + (c_{n_\beta})_{\text{Fuselage}}$, [18].

### 4.2 State Space Representation and Synthesis of the Algorithm

Defining the control input $u = [\dot{F}_1, \dot{F}_2, \dot{F}_3, \dot{F}_4]$, the dynamic model of the quadrotor can be written as two subsystems of the form (1–6) which are coupled by the new control variable $u$ [23]. These subsystems are respectively the underactuated, the fully actuated and the propeller subsystem. Let $x = [x_1, \ldots, x_7]$ be the state for the quadrotor system:

$$x_1 = \begin{bmatrix} x \\ y \end{bmatrix},\ x_2 = \begin{bmatrix} \dot{x} \\ \dot{y} \end{bmatrix}\ x_3 = \begin{bmatrix} \phi \\ \theta \end{bmatrix},\ x_4 = \begin{bmatrix} \dot{\phi} \\ \dot{\theta} \end{bmatrix},$$

$$x_5 = \begin{bmatrix} \psi \\ z \end{bmatrix},\ x_6 = \begin{bmatrix} \dot{\psi} \\ \dot{z} \end{bmatrix},\ x_7 = [F_1, F_2, F_3, F_4]^T \tag{63}$$

Using Eq. 63, let the system (57–58) be rewritten as in state-space form as follows

$$\dot{x}_1 = x_2 \tag{64}$$

$$\dot{x}_2 = f_2(x_2, x_3, x_5, x_6) + g_2(x_5, x_7)\varphi_2(x_3) + d_2 \tag{65}$$

$$\dot{x}_3 = x_4 \tag{66}$$

$$\dot{x}_4 = f_4(x_3, x_4, x_6, x_7) + g_4(x_3)\varphi_4(x_7) + d_4 \tag{67}$$

$$\dot{x}_5 = x_6 \tag{68}$$

$$\dot{x}_6 = f_6(x_3, x_4, x_6, x_7) + g_6(x_3)\varphi_2(x_7) + d_6 \tag{69}$$

$$\dot{x}_7 = u \tag{70}$$

where flow $f_i$, input vectors $g_i$, virtual controls $\varphi_i$ and disturbances $d_i$, for $i = 0, 1, 2$, are given by

$$f_2 = \begin{bmatrix} f_x \\ f_y \end{bmatrix}, \; f_4 = \begin{bmatrix} f_\phi \\ f_\theta \end{bmatrix}, \; f_6 = \begin{bmatrix} f_\psi \\ f_z \end{bmatrix}, \tag{71}$$

$$g_2 = \frac{1}{m}\sum_{i=1}^{4} F_i \begin{bmatrix} s_\psi & c_\psi \\ -c_\psi & s_\psi \end{bmatrix}, g_4 = \begin{bmatrix} \frac{1}{I_x} & \frac{1}{I_y}s_\phi \tau_\theta \\ 0 & \frac{1}{I_y}c_\phi \end{bmatrix} \tag{72}$$

$$g_6 = \begin{bmatrix} \frac{c_\phi}{I_z c_\theta} & 0 \\ 0 & \frac{1}{m}c_\phi c_\theta \end{bmatrix}, \tag{73}$$

$$\varphi_2 = \begin{bmatrix} s_\phi \\ c_\phi s_\theta \end{bmatrix}, \; \varphi_4 = \begin{bmatrix} d(F_2 - F_4) \\ d(F_3 - F_1) \end{bmatrix}, \tag{74}$$

$$\varphi_6 = \begin{bmatrix} c(F_1 - F_2 + F_3 - F_4) \\ F_1 + F_2 + F_3 + F_4 \end{bmatrix}, \tag{75}$$

$$d_2 = \begin{bmatrix} d_x \\ d_y \end{bmatrix}, \; d_4 = \begin{bmatrix} d_\phi \\ d_\theta \end{bmatrix}, \; d_6 = \begin{bmatrix} d_\psi \\ d_z \end{bmatrix}. \tag{76}$$

where:

$$\begin{bmatrix} f_x \\ f_y \\ f_z \end{bmatrix} = -\frac{1}{m} R_t K_t R_t^T \dot{\xi} - G \tag{77}$$

$$\begin{aligned} \begin{bmatrix} f_\phi \\ f_\theta \\ f_\psi \end{bmatrix} &= -(I_T R_r)^{-1} \left( I_T \left( \frac{\partial R_r}{\partial \phi}\dot{\phi} + \frac{\partial R_r}{\partial \theta}\dot{\theta} \right) \dot{\eta} \right. \\ &\quad \left. + K_r R_r \dot{\eta} + (R_r \dot{\eta}) \times (I_T R_r \dot{\eta}) \right) \\ &\quad + \begin{bmatrix} -\frac{c}{I_z} c_\phi t_\theta \sum_{i=1}^{4} (-1)^{i+1} F_i \\ \frac{c}{I_z} s_\phi \sum_{i=1}^{4} (-1)^{i+1} F_i \\ \frac{d}{I_y}\frac{s_\phi}{c_\theta}(F_3 - F_1) \end{bmatrix} \end{aligned} \tag{78}$$

The first subsystem includes Eqs. 64–67 which has the form of Eqs. 1–6 with $n = 4$, then according to the Theorem 1, this subsystem can be stabilized for a position tracking task given by $x_{d1}$ in 2 steps. That is, let following virtual controls be

$$\varrho_1 = \dot{x}_{d1} \tag{79}$$

$$\varrho_2 = g_2^{-1}(x)\left( K_{d1} S_{r1} - \overline{Y}_{r1} \right) \tag{80}$$

$$\varrho_3 = J_3^{-1}(x)\dot{\overline{\varrho}}_2 \tag{81}$$

$$\varrho_4 = \left[ J_3(x) g_4(x) \right]^{-1} \left( K_{d3} S_{r3} - \overline{Y}_{r3} \right) \tag{82}$$

It is important to emphasize that $g_2(x)$ is nonsingular for $F_i \neq 0$, $g_4(x)$ and $J_3(x)$ are nonsingular matrices when $\phi, \theta \neq \pm\frac{\pi}{2}$. The second subsystem consists of Eqs. 68–69 which also has the form of Eqs. 1–6, with $n = 2$, then Theorem 1 suggests that this subsystem can be stabilized at desired reference $x_{d5}$ in one step by the algorithm proposed. In this way, one obtains the following virtual controls

$$\varrho_5 = \dot{x}_{d5} \tag{83}$$

$$\varrho_6 = g_6^{-1}\left( K_{d5} S_{r5} - \overline{Y}_{r5} \right) \tag{84}$$

Finally, the physical control law that stabilize both systems is obtained with the classical backstepping as it is suggested in Remark 1, as follows

$$u = \begin{bmatrix} J_4 \\ J_6 \end{bmatrix}^{-1} \left( A_7 \zeta_7 + \begin{bmatrix} J_3 g_4 & 0 \\ 0 & g_6 \end{bmatrix}^T \begin{bmatrix} S_{r3} \\ S_{r5} \end{bmatrix} + \begin{bmatrix} \dot{\overline{\varrho}}_4 \\ \dot{\overline{\varrho}}_6 \end{bmatrix} \right)$$

where $[J_4^T \; J_6^T]^T$ is a constant nonsingular matrix, therefore $u$ is well posed.

## 5 Simulations

In order to prove the effectiveness of the proposed scheme, three simulation studies are presented to verify the tracking characteristics and robustness against disturbances and parametric uncertainty, as established in Theorem 1.

### 5.1 The Simulator

Simulations are programmed in Matlab® platform with a fixed step numerical Euler integrator, at 1*ms* of step size, in an Intel®-based PC equipped

with Core™ i7-2670QM CPU @ 2.2 GHz × 8 running OS Ubuntu 12.04 and 6Gb of RAM memory.

#### 5.1.1 System Parameters

The parameters of quadrotor considered for simulations are shown in Table 1, which represents approximate conditions found in real flying conditions in a controlled environment.

### 5.2 Simulation Subject to Sideslip Disturbance

#### 5.2.1 Desired Trajectory, Feedback Gains, and Sideslip Aerodynamic Effect

For this simulation, a circumference is considered as desired trajectory, $\left[x_d, y_d, z_d\right]^T = 0.25\left[\sin(\pi t/20) - 1, \cos(\pi t/20), 0.4\right]^T$ m, $\psi_d = -0.016t$ with initial conditions at $\left[x(t_0), y(t_0), z(t_0)\right]^T = \left[-0.25, 0.25, 0\right]^T$ m, $[\phi(t_0), \theta(t_0), \psi(t_0)]^T = [0, 0, 0]^T$ rad. Feedback gains are $A_7 = \text{diag}(60, 60, 60, 60)$, $K_{d_1} = K_{d_3} = \text{diag}(8, 8)$, $K_{d_5} = \text{diag}(12, 12)$, the sliding mode gains are $\gamma_1 = \gamma_3 = \gamma_5 = \text{diag}(0.01, 0.01)$, with $\alpha_1 = \alpha_3 = \alpha_5 = \text{diag}(1, 1)$ and $\kappa_1 = \kappa_3 = \kappa_5 = 3$. Aerodynamic sideslip effect, which is modeled as a saturated smooth piecewise disturbance $\sigma_5(t - 10)$ for $t \geq 10s$, with a magnitude of $5m/s$ and sideslip angle $\beta = \pi/4$ rad, which represents a strong aerodynamic disturbance for this such lightweight quadrotor.

**Table 1** Parameters of quadrotor

| Parameter | Value | Units |
|---|---|---|
| m | 2 | Kg |
| $(I_x, I_y, I_z)$ | (0.1241,0.1241, 0.2483) | Kg m$^2$/rad |
| d | 0.2 | m |
| c | 0.01 | – |
| g | 9.81 | m/s$^2$ |
| $\varrho$ | 1.19 | kg/m$^3$ |
| $K_t$ | 0.01 | Ns/m |
| $K_r$ | 0.001 | Nms/rad |
| $c_l$ | 0.15 | – |
| $c_m$ | 0.25 | – |
| $c_n$ | 0.8 | – |
| $c_L$ | 0.4 | – |
| $c_Y$ | 0.2 | – |
| $c_D$ | 0.1 | – |
| S | 0.5 | m$^2$ |
| b | 0.05 | m |
| $\bar{c}$ | 0.02 | m |

#### 5.2.2 Results

Tracking of position shows rejection of disturbances from the invariance of the sliding surface, despite the underactuation structure, with imperceptible errors in the vicinity of the origin, and convergence of attitude coordinates, where the actual yaw angle tracks satisfactorily the desired time-varying reference (Fig. 3). Chattering free thrust is shown in Fig. 4, where it can be seen the effort to compensate disturbance at $t \geq 10s$.

### 5.3 Simulation Study Subject to Wind Gust

#### 5.3.1 Desired Trajectory, Feedback Gains, and Wind Gust Effect

It is considered a smooth displacement of $2m$ at $z$-axis with $\psi_d = 0$ and zero initial conditions. All feedback gains are the same as those in Section 5.2. Wind gust is simulated by 3 disturbances at time 3 s, 5.5 s and 8 s as Gaussian functions with standard deviation of 0.15, with a wind vector $v_{\text{wind}} = [2.5,\ 2.5,\ 1.25]^T$ m/s.

#### 5.3.2 Results

Wind gust does not affect significantly the tracking of position, as shown in Fig. 5, with attitude coordinates in a vicinity of the origin. Figure 6 shows thrust of each actuator, reduced when the wind gust is present due to its $z$ component and the chattering free activity remains despite the disturbance.

### 5.4 Simulation Study under Parametric Uncertainty

#### 5.4.1 Desired Trajectory, Feedback Gains, and Parametric Uncertainty

It is considered a desired trajectory $\psi_d = -0.1t$,

$$\left[x_d, y_d, z_d\right]^T = 0.5\left[\sin(2\pi t/15) - 1, \cos(2\pi t/15), 0.1t\right]^T \text{m}$$

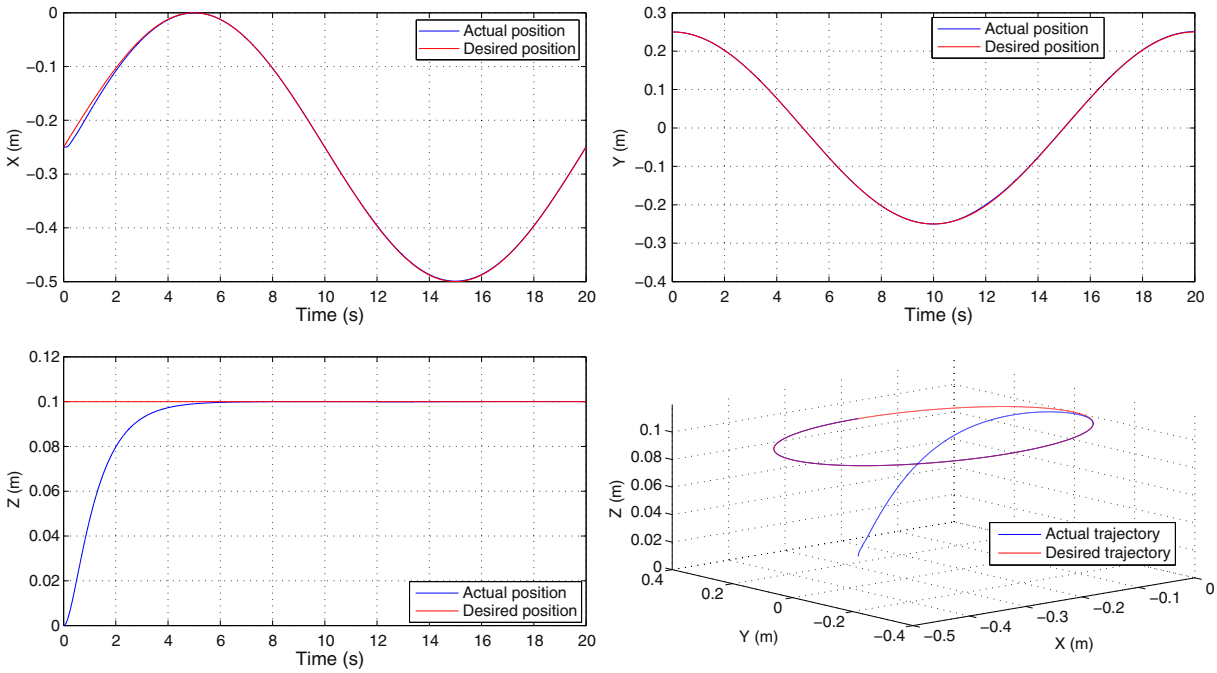


**Fig. 3** Desired and actual Cartesian position of quadrotor under sideslip effect

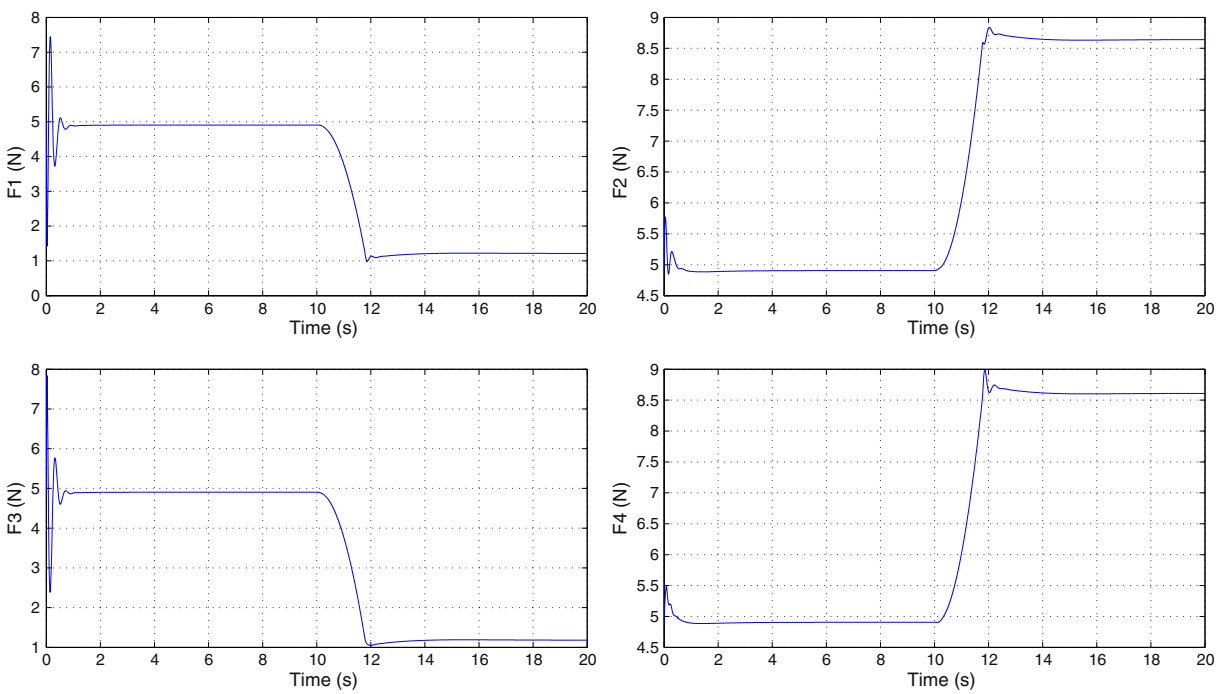


**Fig. 4** Thrust of each actuator are chatterless, and smooth at $t \geq 10s$, when disturbances is present

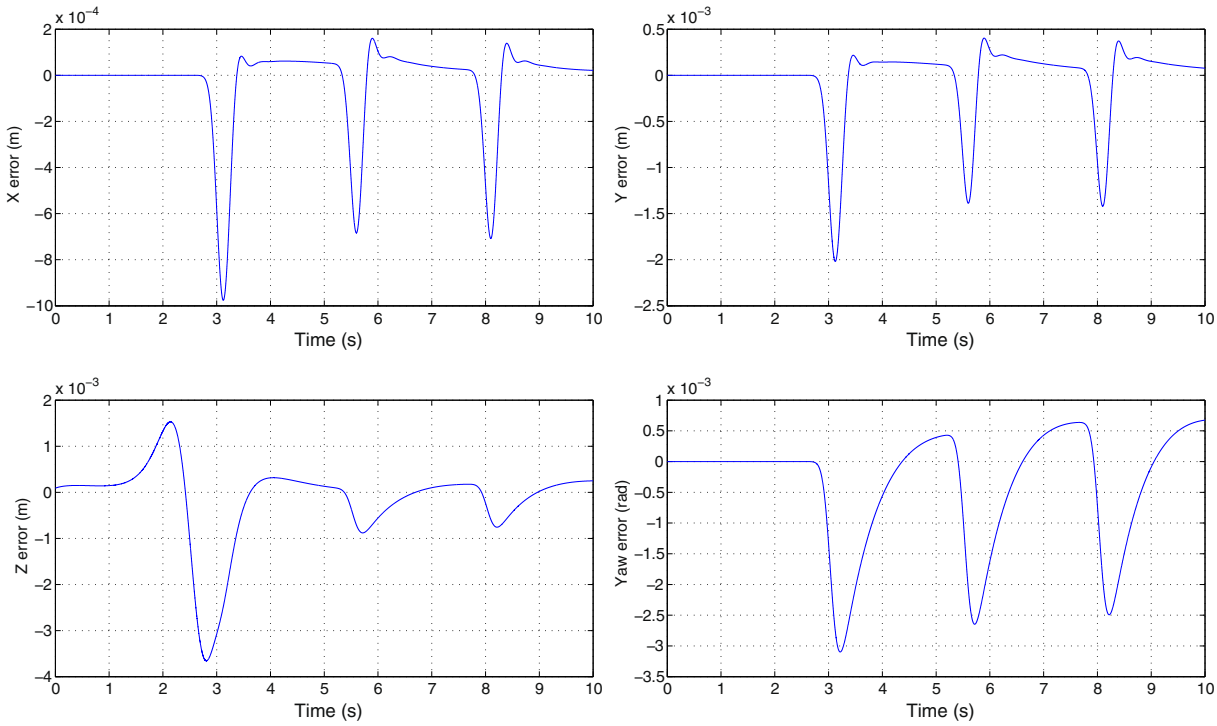


**Fig. 5** Error variables of tracking task for quadrotor. Control maintains the error variables enough small under wind gust

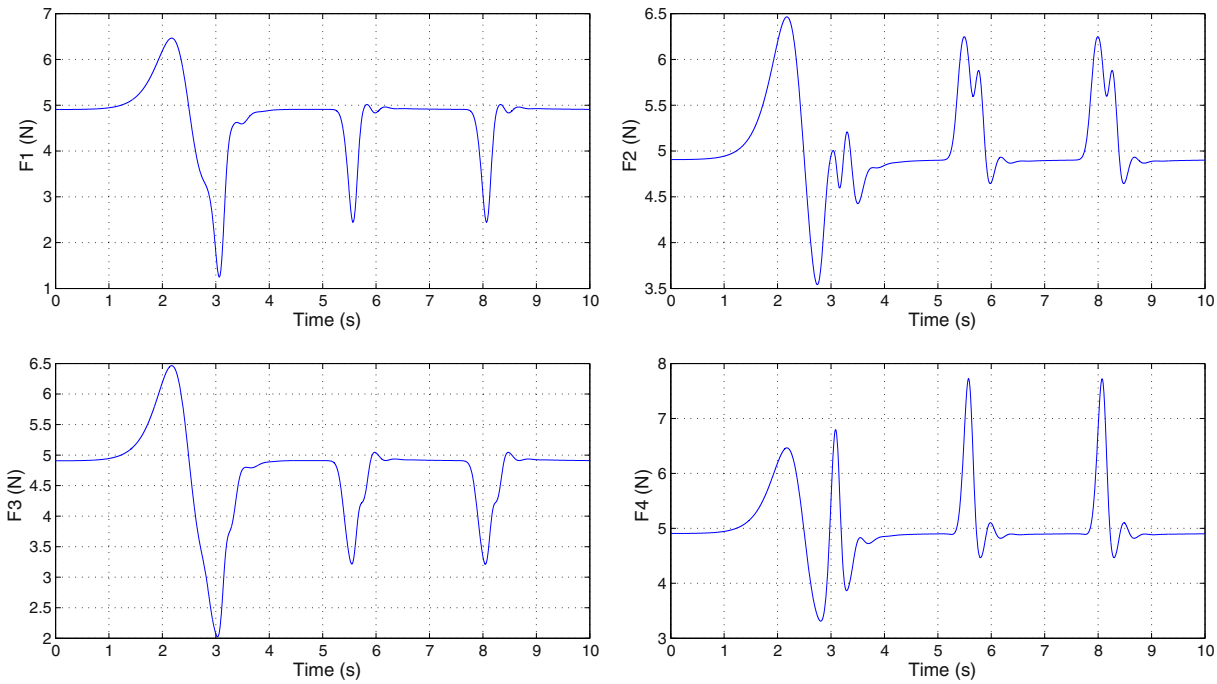


**Fig. 6** Thrust of each actuator is chatterless, and smooth. At $t = 3s$, $5.5s$ and $8s$ the thrust is reduced due to the positive $z$ component of the wind

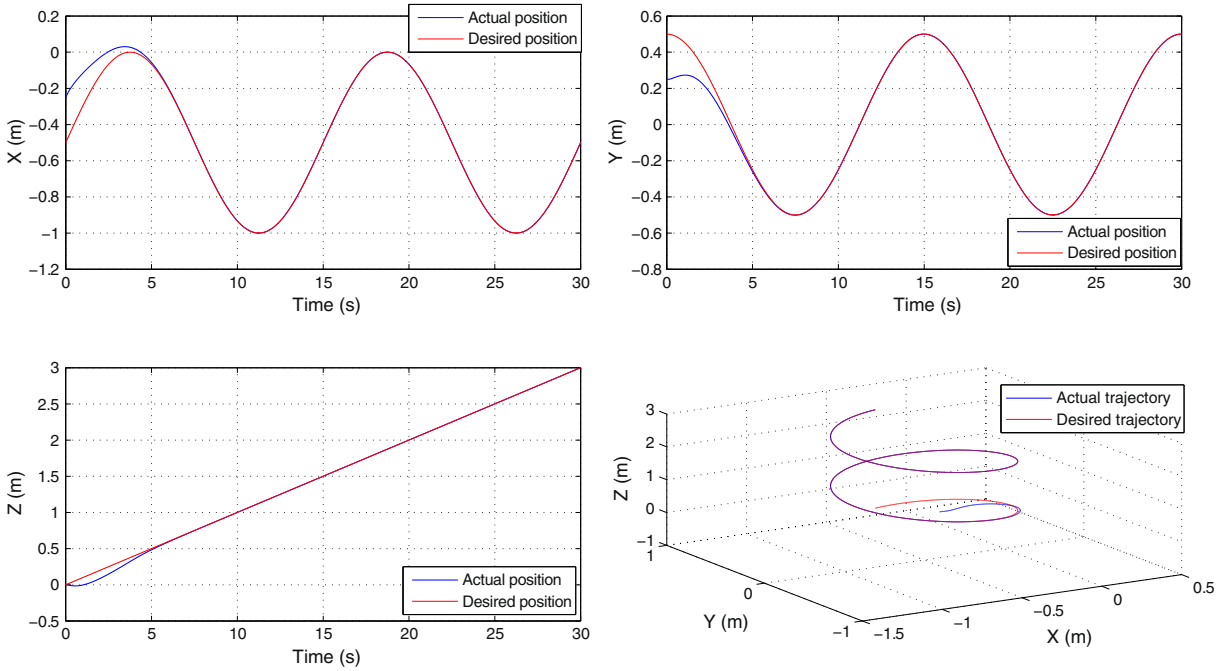


**Fig. 7** Position of quadrotor under parametric uncertainty

with initial conditions at $[x(t_0), y(t_0), z(t_0)]^T = [-0.25, 0.25, 0]^T$, $[\phi(t_0), \theta(t_0), \psi(t_0)]^T = [0, 0, 0]^T$. Feedback gains are $A_7 = \text{diag}(60, 60, 60, 60)$, $K_{d_1} = \text{diag}(1.6, 1.6)$, $K_{d_3} = \text{diag}(4, 4)$, $K_{d_5} = \text{diag}(24, 24)$, the sliding mode gains are $\gamma_1 = \gamma_3 = \gamma_5 = \text{diag}(0.05, 0.05)$, with $\alpha_1 = \alpha_3 = \alpha_5 = \text{diag}(1, 1)$

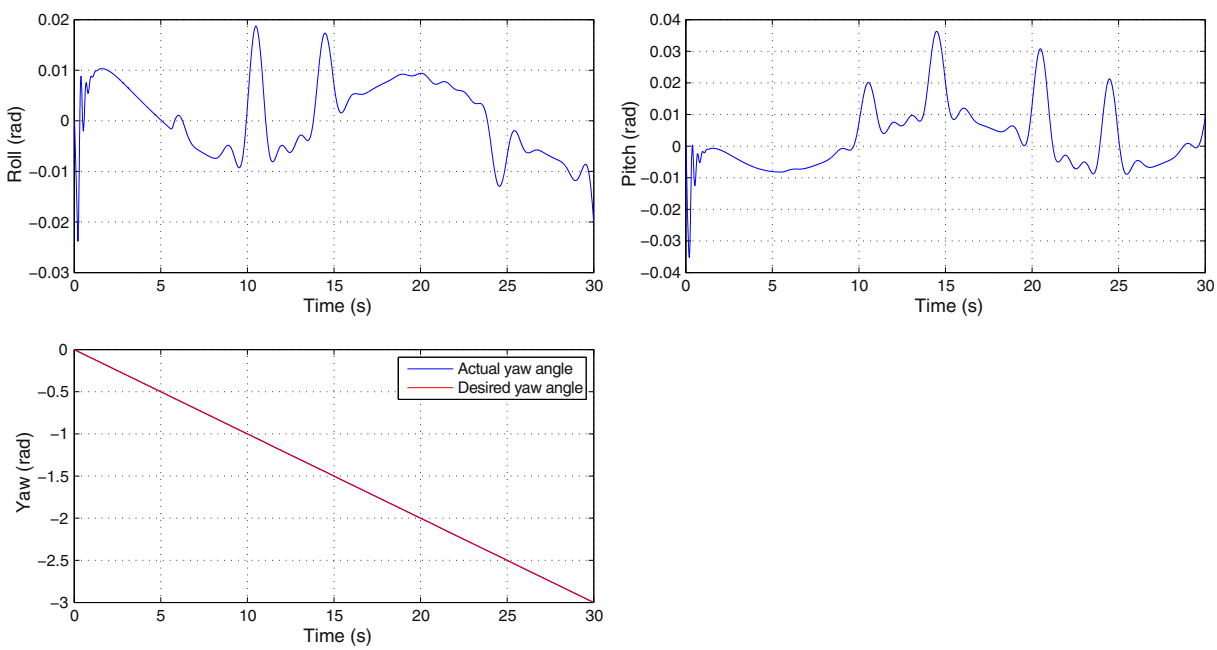


**Fig. 8** Attitude of quadrotor under parametric uncertainty

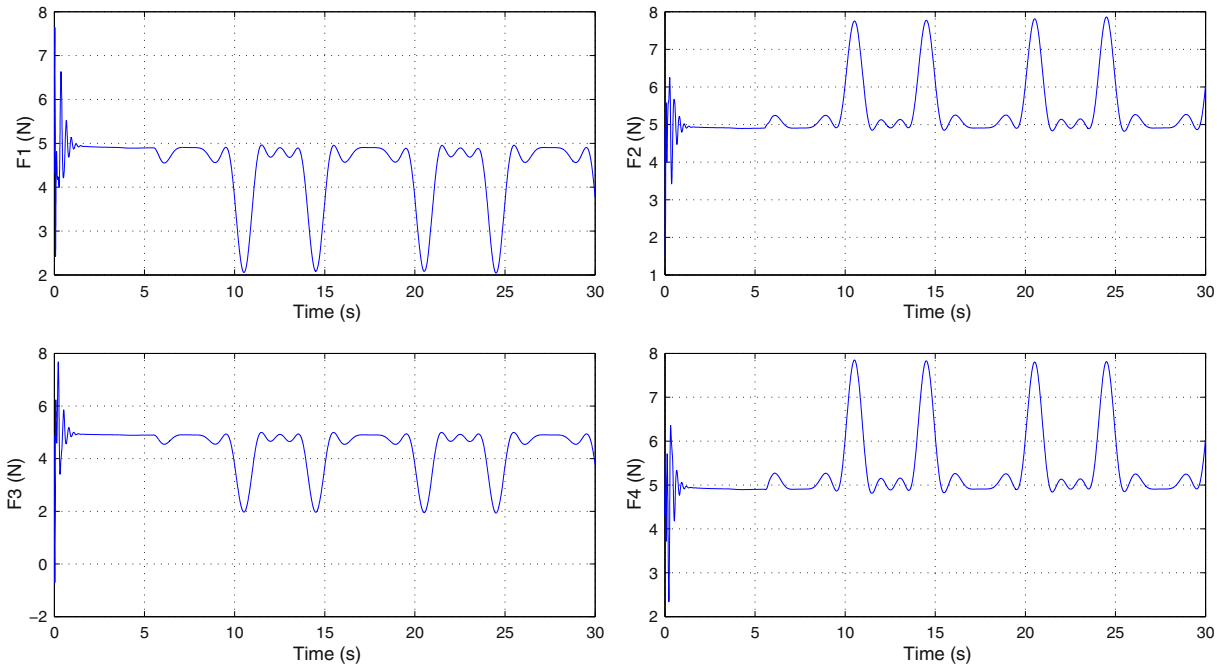


**Fig. 9** Thrust of each actuator is chatterless, and smooth under parametric uncertainty

and $\kappa_1 = \kappa_3 = \kappa_5 = 1$. In this simulation a parametric uncertainty of $-25\%$ was considered for parameters $m$, $I_x$, $I_y$, $I_z$, $d$, $c$, $K_t$, $K_r$ and $g$, while the quadrotor is subject to a wind disturbance with the velocity $v_{\text{wind}} = \sin(0.8\pi t) + \cos(0.2\pi t) + \sin(0.4\pi t) + \cos(0.6\pi t)\,[1,\ 1,\ 0]^T$ m/s after 5.5 s.

*5.4.2 Results*

In Fig. 7, the position of the quadrotor is shown, the tracking task is accomplished satisfactorily, that is, the neglected dynamics given by the parametric uncertainty and unmatched disturbances are rejected by the proposed control law, while the attitude parameters of the quadrotor remain stable as is shown in Fig. 8.

The control signals for each actuator are shown in Fig. 9, these signals are smooth and the greater effort is at the beginning in order to compensate the parametric uncertainty and after 5.5 s when the aerodynamic disturbance is present.

## 6 Conclusions

A constructive approach based on backstepping and a novel error frame that involves the integral of the *signum* of the sliding surface are proposed to solve the underactuation problem without chattering for nonlinear underactuated plants. It resorts on the systematic backstepping control design, yet the proposed modification allows an inner control loop to compensate for bounded disturbances and parametric uncertainties with a chattering-free control effort through integral sliding modes. This approach can be applied to a number of plants that can be converted into the cannonical forms under consideration, which covers a wide number of plants, however it has been motivated by the quadrotor problem. Stability in the sense of Lyapunov is derived and invariance, to output error dynamics, is proved based on the usual concepts of variable structure systems. An illustrative simulation study is discussed in detail for the quadrotor aerial underactuated robot system under various conditions, subject to aerodynamic disturbances. It is shown that this plant in particular can be written as the interconnection of three subsystems, similar to Unmanned Underwater Vehicles. This backstepping-based controller conveys an intuitive solution for underactuation by commanding the actuated subsystem in a extended error coordinate system, where

uncertainties are compensated. The integral sliding mode for the actuated block provides realization of the virtual controller needed to stabilize the underactuated subsystem, which shows the viability of the proposed approach for a wide variety of plants.

## References


1. Krstic, M., Kanellakopoulos, I., Kokotovic, P.V.: Nonlinear and Adaptive Control Design. Wiley, New York (1995)
2. Jafari Koshkouei, A., Zinober, A.-S.-I.: Adaptive sliding backstepping control of nonlinear semi-strict feedback form systems. In: Proc. of the 7th Mediterranean Conf. on Control and Automation, pp. 2376–2386 (1999)
3. Skjetne, R., Fossen, T.: On integral control in backstepping: Analysis of different techniques. In: Proc. American Control Conf., vol. 2, pp. 1899–1904 (2004)
4. Cunha, R., Cabecinhas, D., Silvestre, C.: Nonlinear trajectory tracking control of a quadrotor vehicle. In: European Control Conf. (2009)
5. Das, A., Lewis, F., Subbarao, K.: Backstepping approach for controlling a quadrotor using Lagrange form dynamics. J. Intell. Robot. Syst. **56**(1–2), 127–151 (2009)
6. Zhang, T., Ge, S.S., Hang, C.C.: Adaptive neural network control for strict-feedback nonlinear systems using backstepping design. In: American Control Conf., vol. 2, pp. 1062–1066 (1999)
7. Bartolini, G., Ferrara, A., Giacomini, L., Usai, A.: Properties of a combined adaptive/second-order sliding mode control algorithm for some classes of uncertain nonlinear systems. IEEE Trans. Autom. Control **45**(7), 1334–1341
8. Isidori, A., Marconi, L., Serrani, A.: Robust nonlinear motion control of a helicopter. IEEE Trans. Autom. Control **48**(3), 413–426
9. Bouabdallah, S., Siegwart, R.: Backstepping and sliding-mode techniques applied to an indoor micro quadrotor. In: 2005 IEEE International Conf. on Robotics and Automation, pp. 2247–2252
10. Gu, W.-J., Zhao, H., Pan, Ch.: Sliding mode control for an aerodynamic missile based on backstepping design. J. Control Theory Appl. **1**, 71–75 (2005)
11. Swaroop, D., Hedrick, J.K., Yip, P.P., Gerdes, J.C.: Dynamic surface control for a class of nonlinear systems. IEEE Trans. Autom. Control **45**(10), 1893–1899 (2000)
12. Nersesov, S.-G., Ashrafiuon, H., Ghorbanian, P.: On the stability of sliding mode control for a class of underactuated nonlinear systems. In: 2010 American Control Conf., pp. 3446–3451
13. Bouadi, H., Bouchoucha, M., Tadjine, M.: Sliding Mode Control based on Backstepping Approach for an UAV Type-Quadrotor. World Acad. Sci. Eng. Technol. **2**, 22–27 (2007)
14. Luque-Vega, L., Castillo-Toledo, B., Loukianov, A.G.: Robust block second order sliding mode control for a quadrotor. J. Frankl. Inst. **349**, 719–739 (2012)
15. Levant, A.: Robust exact differentiation via sliding mode technique. Automatica **34**(3), 379–384 (1998)
16. Madani, T., Benallegue, A.: backstepping control with exact 2-sliding mode estimation for a quadrotor unmanned aerial vehicle. In: 2007 IEEE/RSJ Int. Conf. on Int. Robots and Systems, pp. 141–146
17. Parra-Vega, V., Arimoto, S., Liu, Y.-H., Hirzinger, G., Akella, P.: Dynamic sliding pid control for tracking of robots manipulators: theory and experiments. IEEE Trans. Robot. Autom. **19**(6), 967–976 (2003)
18. Stengel, R.F.: Flight Dynamics. Princeton University Press (2004)
19. Leishman, J.G.: Principles of Helicopter Aerodynamics. Cambridge University Press, Cambridge, MA (2006)
20. Bazov, D.I.: Helicopter Aerodynamics. NASA, Washington (1972)
21. Koo, T.J., Sastry, S.: Output tracking control design of a helicopter model based on approximate linearization. In: Proc. IEEE Conf. on Decision and Control, pp. 3635–3640 (1998)
22. Frazzoli, E., Dahleh, M., Feron, E.: Trajectory tracking control design for autonomous helicopters using a backstepping algorithm. In: Proc. American Control Conference, vol. 6, pp. 4102–4107 (2000)
23. Madani, T., Benallegue, A.: Backstepping control for a quadrotor helicopter. In: Proceedings of the 2006 IEEE/RSJ International Conference on Intelligent Robots and Systems, pp. 3255–3260 (2006)